Exploring the Origins of UHECRs : Insights from Simulated Relativistic Jets

Jeongbhin Seo* & Dongsu Ryu (Ulsan National Institute of Science & Technology)

Hyesung Kang (Pusan National University)

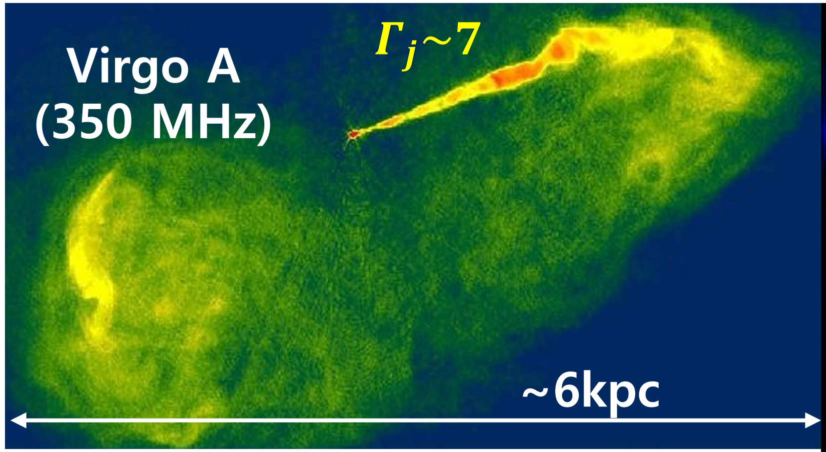

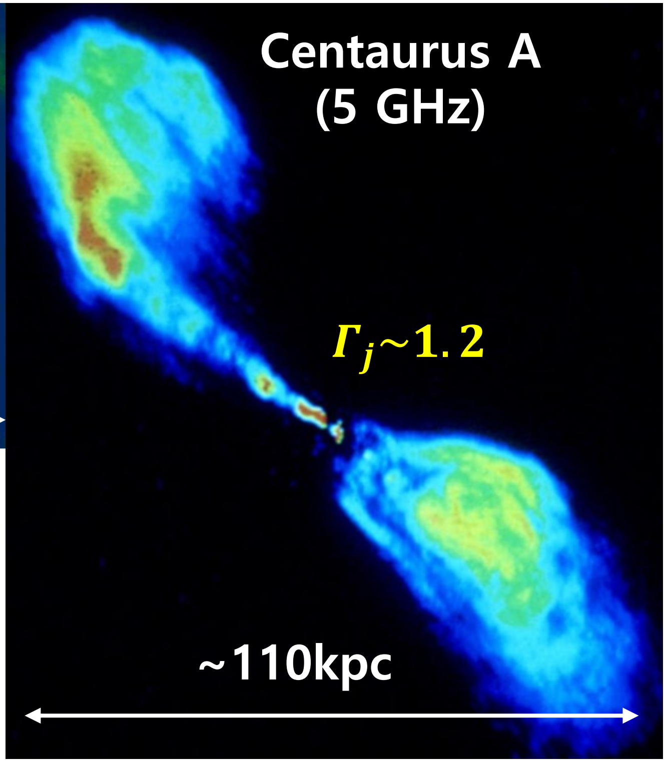

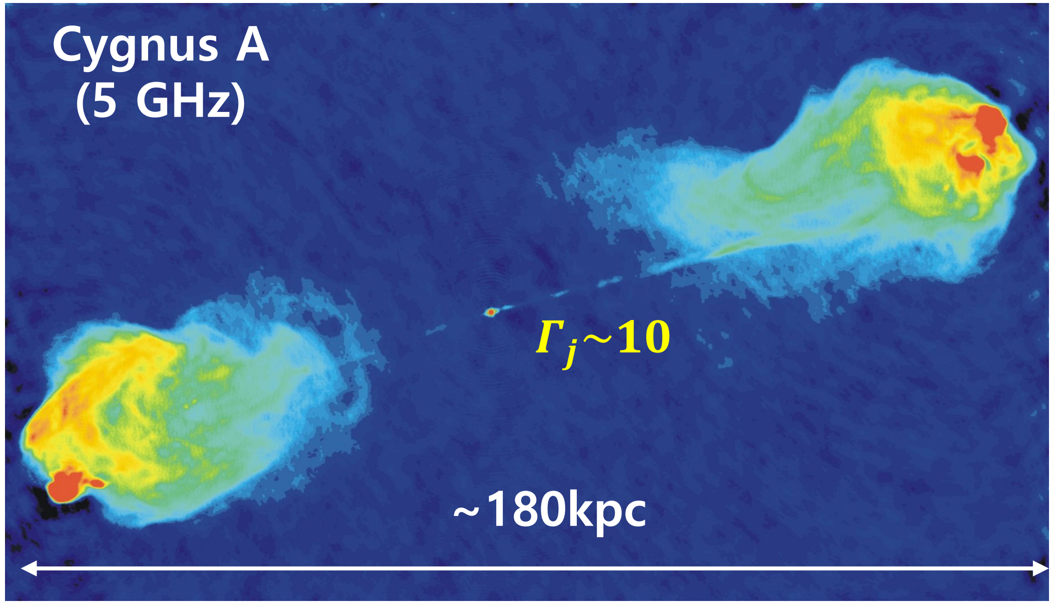

-core
-one-sided relativistic jet
-outer lobes (+hot spots)

Jets & Lobes of Giant Radio galaxies: acceleration sites of UHECRs

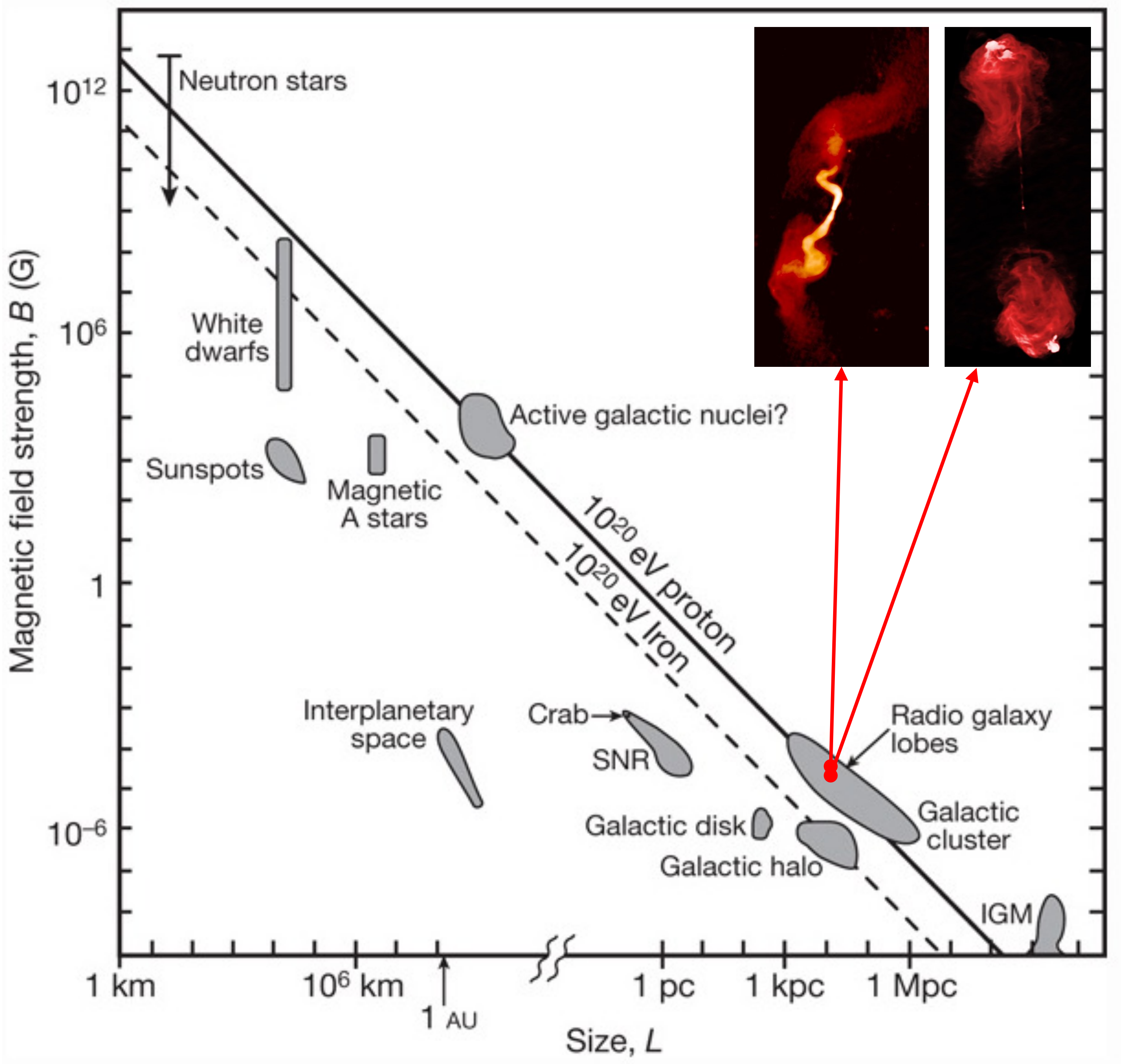

Hillas criteria: confinement condition

Particles should be confined within accelerator in order to be accelerated. $r_g \leq L$

$$E_{\mathrm{Hillas}}(\mathrm{EeV}) \leq \beta_a \cdot B_{\mu G} L_{\mathrm{kpc}}$$ for proton

$$E_{Z_i,\mathrm{Hillas}} = Z_i E_{\mathrm{Hillas}}$$ For heavy ions

Z_i =charge $\quad \beta_a = V_a/c \quad B_{\mu G} = \frac{B}{1\mu G} \quad L_{\mathrm{kpc}} = \frac{L}{1kpc}$

Relativistic jets on 10-100 kpc scales:

FR-I : $\Gamma_j \sim 1 - 10, \quad Q_j \leq 10^{45}$ erg/s

FR-II : $\Gamma_j \geq 10, \quad Q_j \geq 10^{45}$ erg/s

Most promising candidate for UHECR sources

(Ostrowski 1998, Caprioli 2015, Kimura et al. 2018; Rieger 2019; Matthews et al. 2019; Rachen et al 2019, Hardcastle & Croston 2020; + many previous studies)

Two steps: Quantitative numerical estimation of UHECR acceleration in RG jets

Relativistic hydrodynamic (RHD) simulations of relativistic jets with $\Gamma_j \sim 1-70$ Seo et al. 2021b

→ Models for
1. B field amp
2. $\lambda_{\mathrm{mfp}} \propto p^{\delta}$

\+ **Monte Carlo simulations** of the CR transport in simulated jet-induced flows.

Seo et al. 2023 a, b

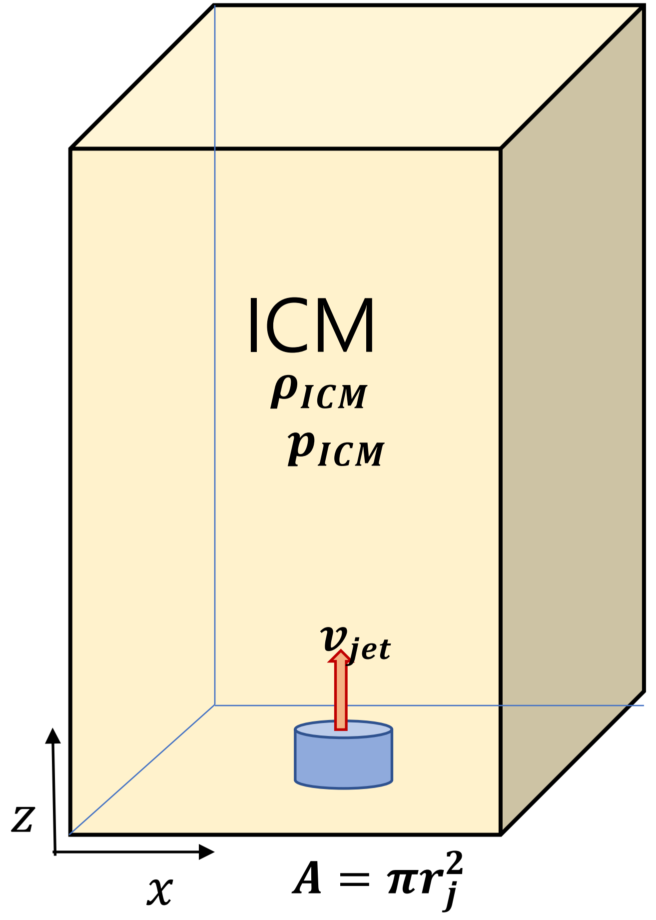

HOW(High-Order WENO)-RHD code (Seo et al 2021a):

-5th order WENO scheme
-4th order SSPRK time integration
-Realistic Equation of State: RC (Ryu et al. 2006)
-transverse flux averaging
-modified eigenvalues

Jet Power: $$Q_j = \pi r_j^2 v_j (\Gamma_j^2 \rho_j h_j - \Gamma_j \rho_j c^2)$$

depends on Γ_j, r_j, ρ_j, p_j of the jet inflow

$$r_j = 10\mathrm{pc} - 1\mathrm{kpc}, \quad \Gamma_j \sim 1-70, \quad Q_j \sim 10^{42} - 10^{47} \mathrm{erg/s}$$

Flow structures of simulated relativistic jets

Jet Power: $Q_j = \pi r_j^2 v_j (\Gamma_j^2 \rho_j h_j - \Gamma_j \rho_j c^2)$: **key parameter** that governs the jet dynamics

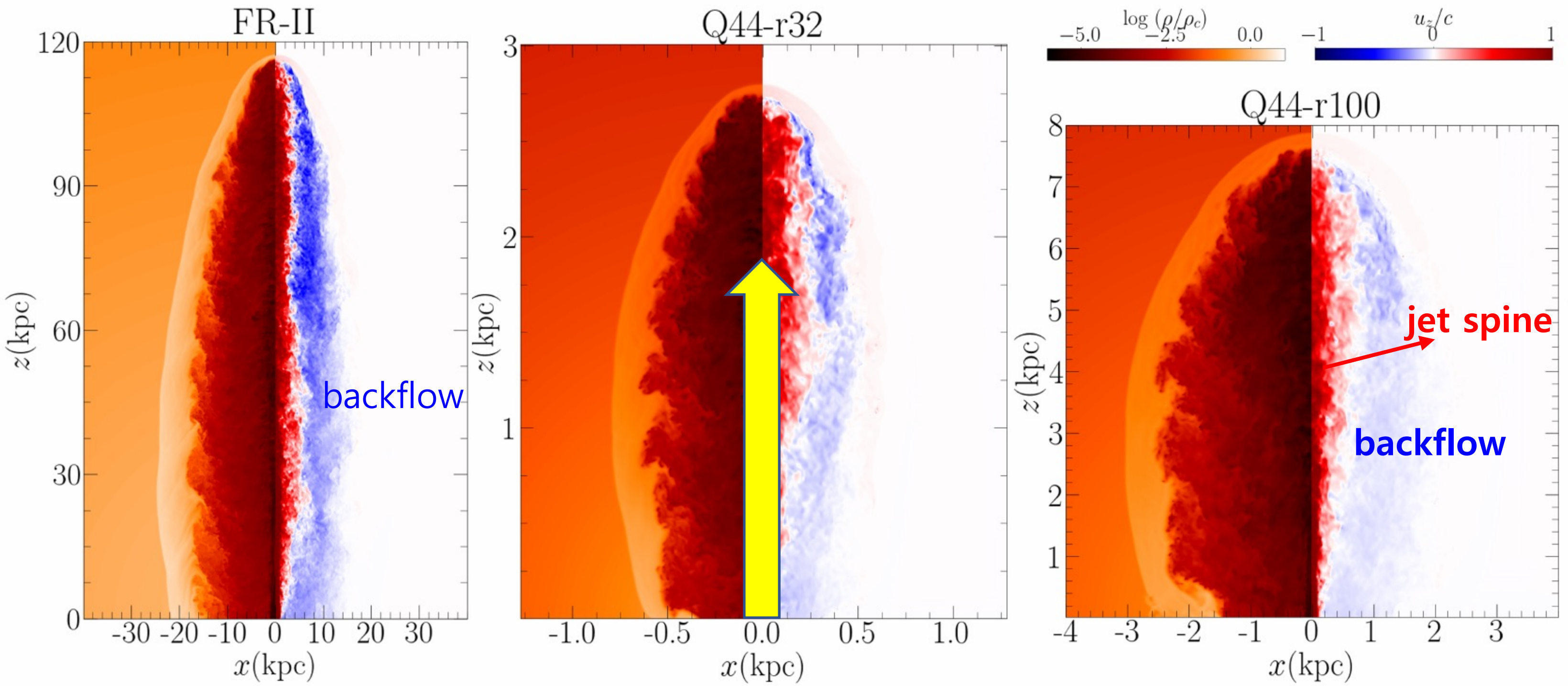

deceleration of jet-spine flow

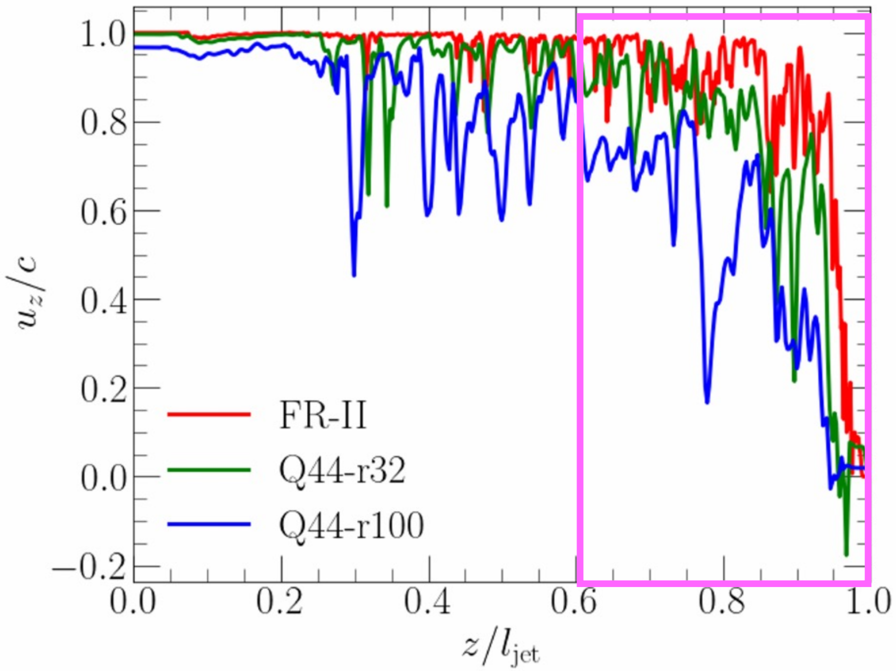

$\Gamma_j \sim 23$
$r_j = 1$ kpc
$Q_j \sim 3.3\times10^{46}$ erg/s
$\langle\Gamma\rangle_{\rm spine} \sim 10.3$

$\Gamma_j \sim 11$
$r_j = 32$ pc
$Q_j \sim 3.5\times10^{44}$ erg/s
$\langle\Gamma\rangle_{\rm spine} \sim 5.8$

$\Gamma_j \sim 3.9$,
$r_j = 100$ pc
$Q_j \sim 3.5\times10^{44}$ erg/s
$\langle\Gamma\rangle_{\rm spine} \sim 2.7$

Averaging for $[z] = 0 - \frac{2}{3} l_{jet}$

Low-power jets with smaller Γ_j
→ significant deceleration of the jet-spine flow
→ well developed cocoon

RHD simulations of relativistic jets: shocks, shear, turbulence

Limitations: 1. not MHD simulations

2. MHD turbulence, $\delta B/B$ on subgrid scales not resolved

Vertical vel. vs density

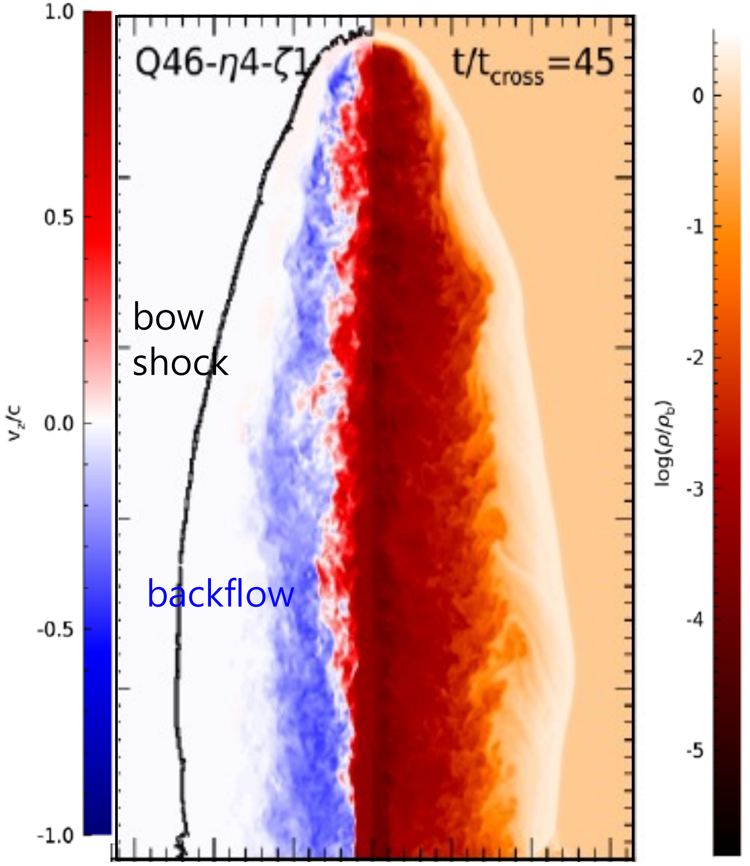

Shock Mach no.

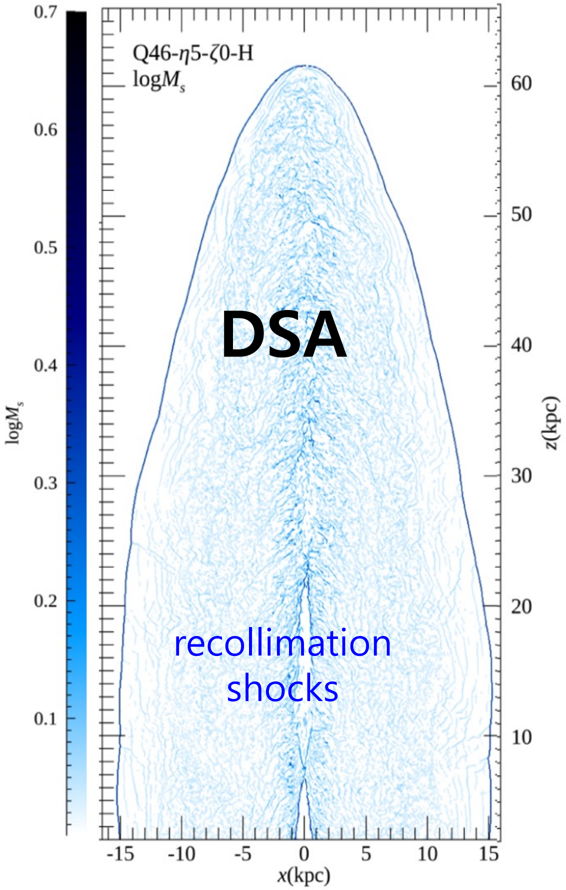

Matthews et al. 2019

Relativistic shear coefficient

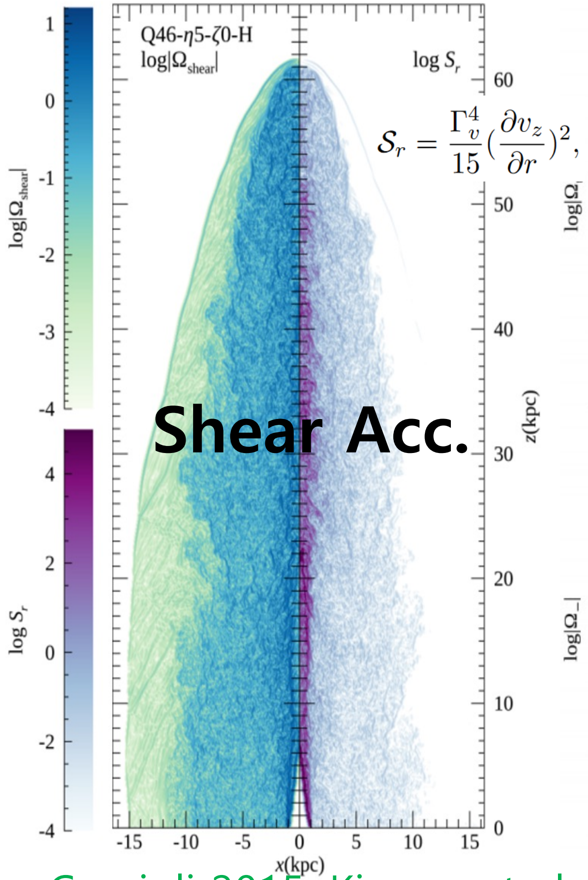

Caprioli 2015, Kimura et al. 2018 Rieger 2019,

Vorticity = turbulence

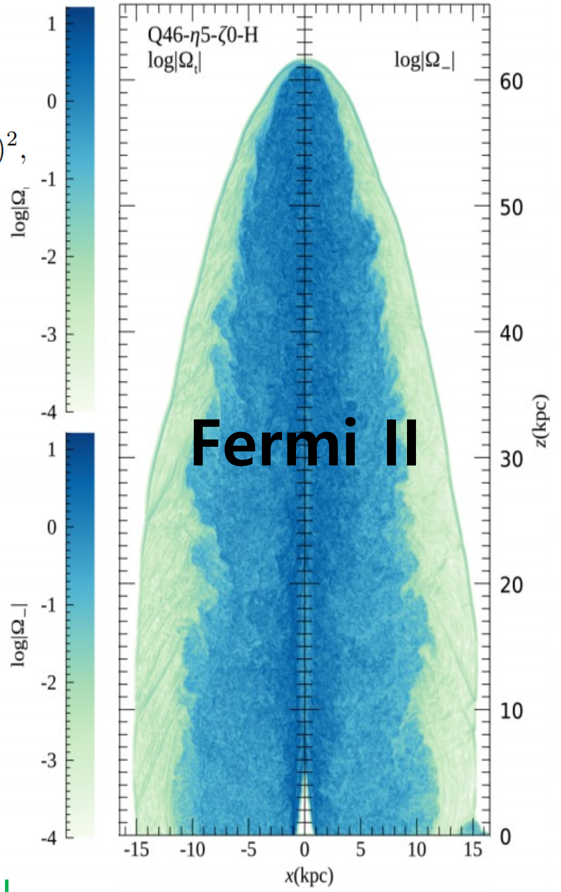

Hardcastle 2010

Characteristic Properties in Different Regions

Parameters	jet spine	backflow	shocked-ICM
$\beta_s = v_s/c$	~ 0.4	$\sim 0.06 - 0.2$	~ 0.01
$\mathcal{L}_{\rm shock}/Q_j$	~ 0.3	~ 0.4	~ 0.03
$\Omega_{\rm shear}/(c/r_j)$	~ 1.5	~ 0.3	~ 0.004
$S_r/(c/r_j)^2$	~ 0.2	~ 0.004	-
$\Omega_-/(c/r_j)$	~ 2.5	~ 0.7	~ 0.005
$\mathcal{L}_{\rm turb}/Q_j$	~ 0.04	~ 0.2	~ 0.02

- Shocks in jet-spine flow are relativistic, while those in backflow are subrelatativistic.
- Shocks formed in jet-spine flow and backflow are most effective in dissipating the jet kinetic energy.
- Turbulence dissipation is most important in backflow.

Seo et al. 2021b

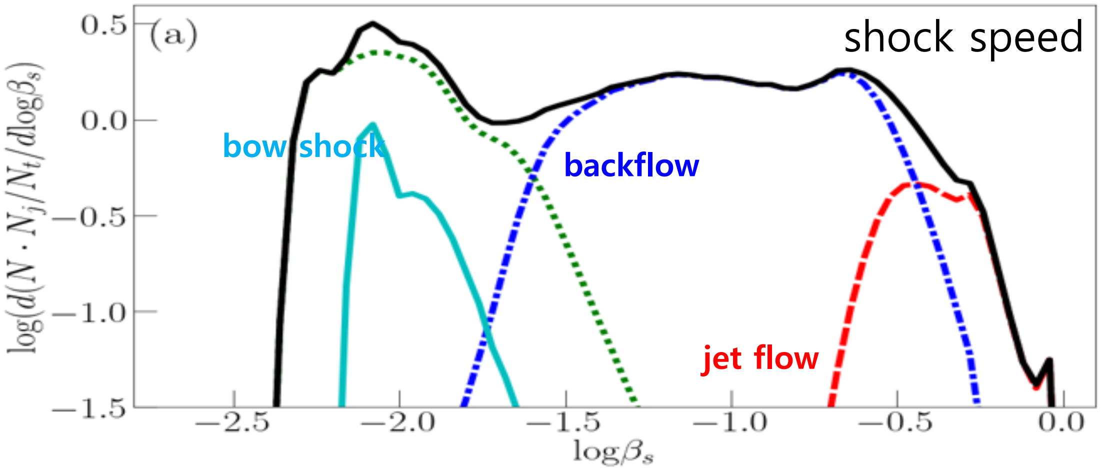

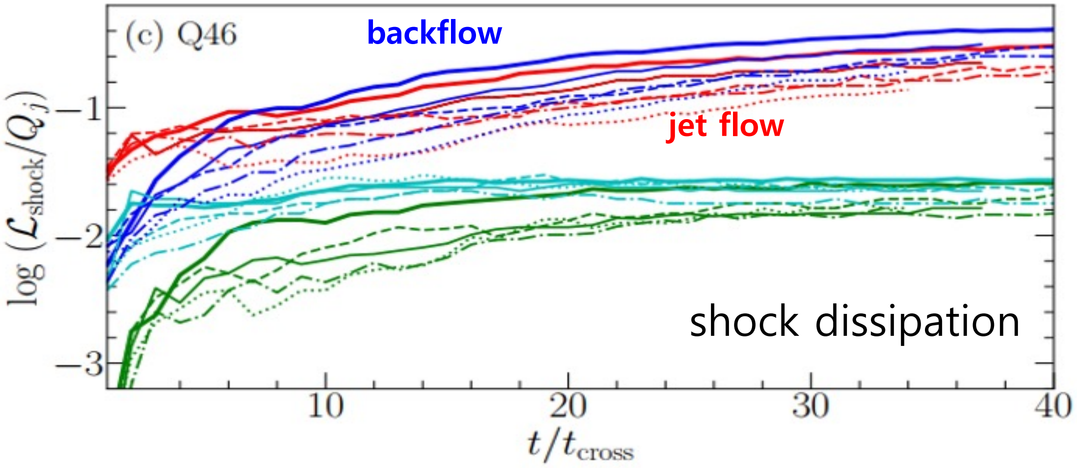

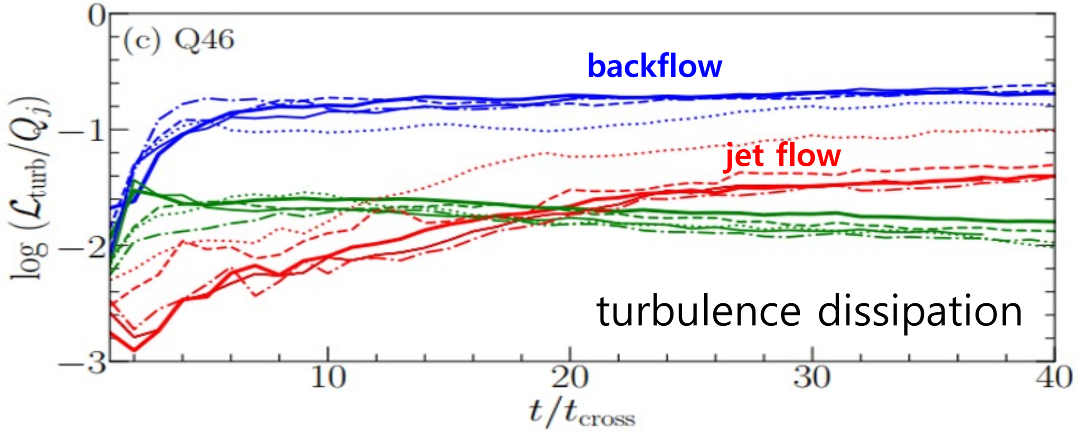

Monte Carlo simulations for CR transport & acceleration

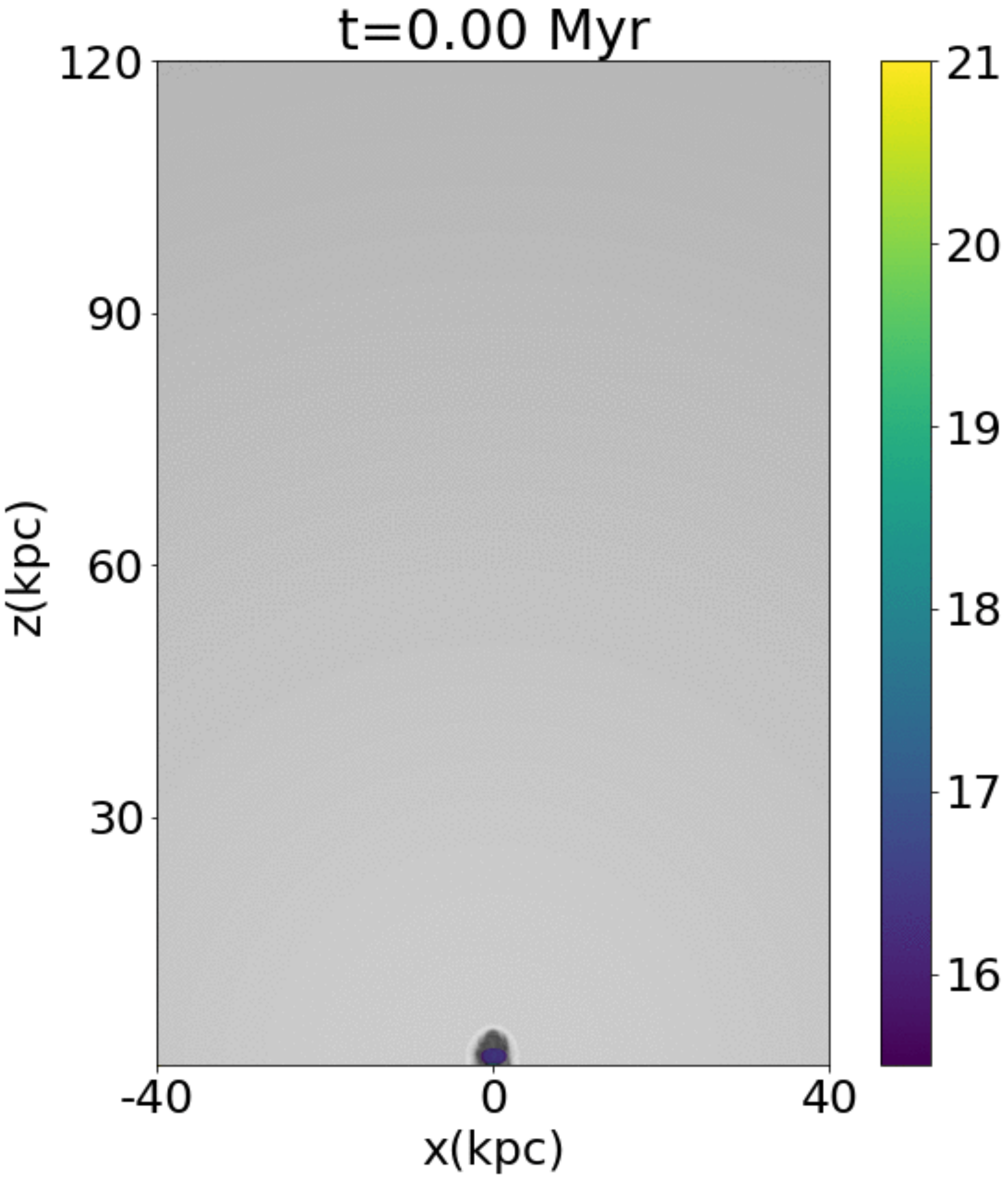

Seo et al. 2023a, b

- seed CRs are injected from the host galaxy through the jet nozzle with a radius r_j
- Initially, seed CRs : $10^{13\text{-}15}$eV with a power-law spectrum $dN/dE \propto E^{-2.7}$.
- Particles are continuously advected & energized in the time-evolving jet flows

Galactic cosmic rays are advected with jet inflow

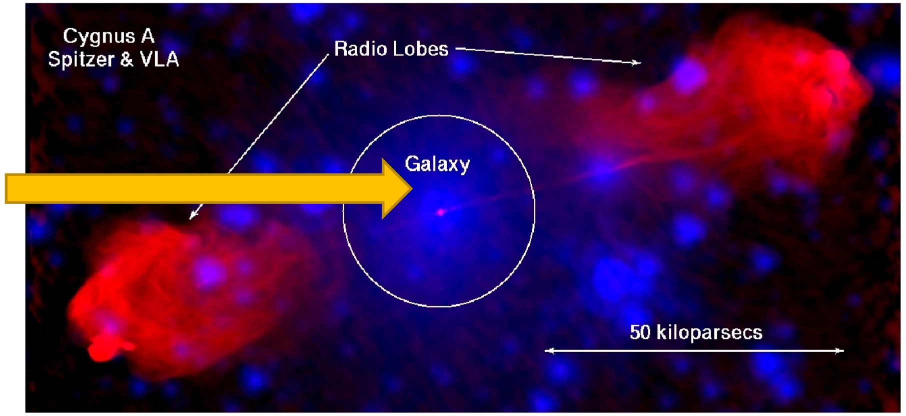

Prescriptions for magnetic field strength

- **Internal energy model**

$$P_B = \frac{B_p^2}{8\pi} = \frac{P}{\beta_p}$$

$\beta_p \approx 100$ plasma beta

- **Turbulence kinetic energy model**

$$\frac{B_{\rm turb}^2}{8\pi} \approx \mathcal{E}_{\rm turb}$$

$$\mathcal{E}_{\rm turb} = \Gamma_{\rm turb}(\Gamma_{\rm turb} - 1)\rho c^2$$

- **Shock amplification model via Bell instability**

$$\frac{B_{Bell}^2}{8\pi} \approx \frac{3}{2}\frac{v_s}{c}P_{CR} \approx \frac{3}{2}\frac{v_s}{c}(0.1\rho_1 v_s^2)$$

$$\Rightarrow \quad B_{\rm comov} = \max(B_p, B_{\rm turb}, B_{\rm Bell})$$

$B_{\rm obs} \approx \Gamma B_{\rm comov}$ in the simulation frame

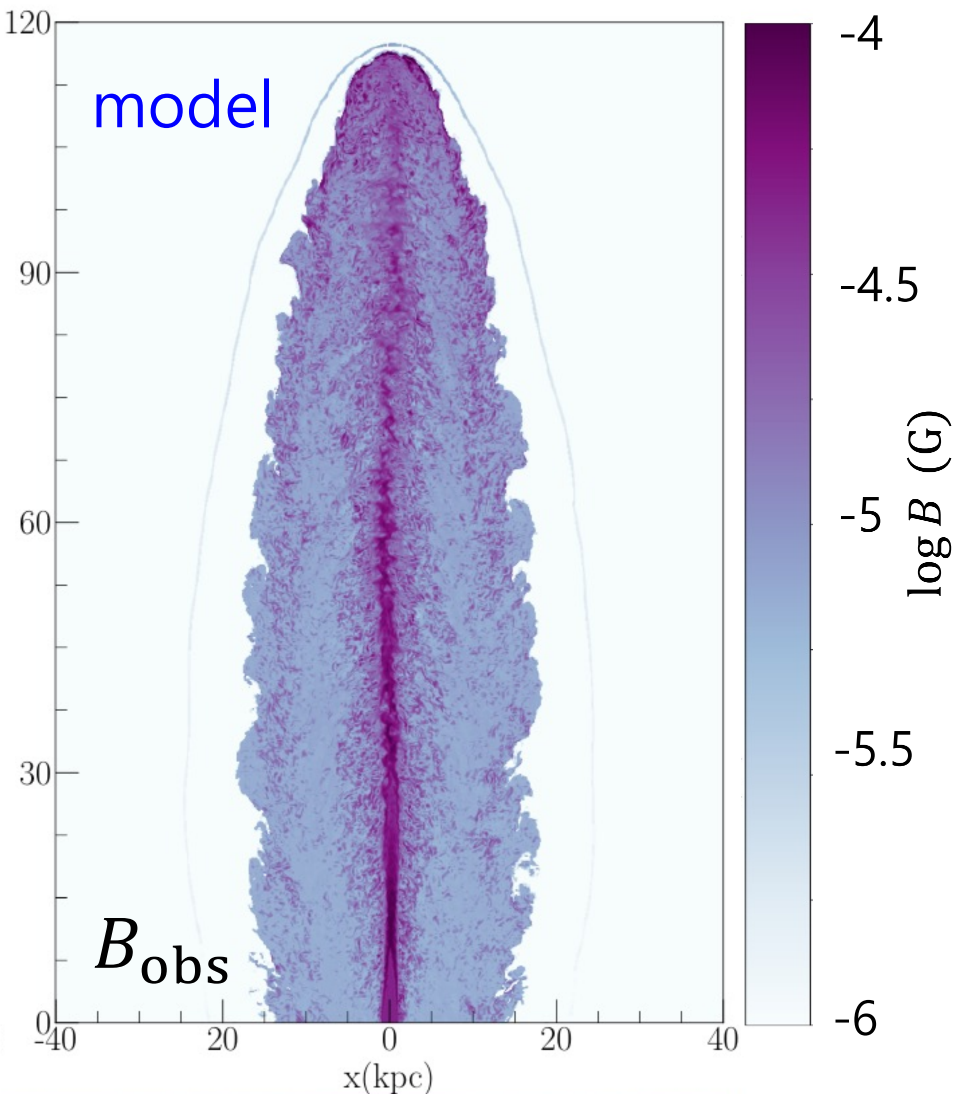

in the computational frame

Jet spine: B ~ $100\mu G$
Backflow: B ~$10\mu G$
ICM: B ~$1\mu G$

Prescriptions for Particle Scattering

mean free path: $\lambda_{\rm mfp} \propto E^{\delta}$

- $\boldsymbol{E < E_{coh}}$: $E_{coh} = eZ_iBL_0$
  due to **turbulence with Kolmogorov spectrum**

➔ $\lambda_{\rm mfp} \propto E^{\frac{1}{3}}$

- $\boldsymbol{E > E_{coh}}$: **Bohm scattering**

➔ $\lambda_{\rm mfp} \propto E$

Bohm scattering at shock zones
due to **self-generated waves** **near shocks**.

Comparison model

$\boldsymbol{E > E_{coh}}$: **non-resonant scattering**

➔ $\lambda_{mf} \propto E^2$

e.g Kimura et al. 2018

Restricted random walk model

In realistic jet flows, there may not be magnetic fluctuations strong enough to scatter in a fully random walk manner for high-energy particles.

$$\delta\theta_{max} = \pi \cdot \min[1, \sim\frac{L_0}{\lambda_f}]$$

-**Forward-beamed scattering** for HE particles

$$\lambda_f(E) \gg L_0 \qquad \delta\theta_{\rm max} \ll 1.$$

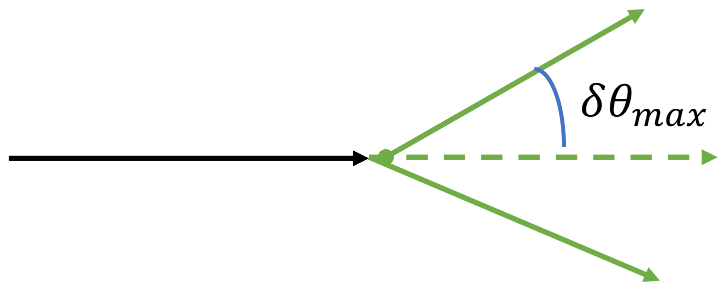

-**Fully isotropic scattering** for LE particles

$$\lambda_f(E) \ll L_0 \quad \delta\theta_{\rm max} \approx \pi.$$

Acceleration Timescales: shock, shear, turbulence

DSA (shock)

$$t_{\rm DSA} = 3.52\times10^3{\rm yr}\frac{\chi(\chi+1)}{\chi-1}\left(\frac{v_s}{c}\right)^{-2}\left(\frac{E}{\rm EeV}\right)\left(\frac{B}{1\mu{\rm G}}\right)^{-1}$$

Drury 1983

Gradual Shear Acc

$$t_{\rm GSA} = 4.90\times10^4{\rm yr}\frac{1}{(4+\alpha)\gamma^4}\left(\frac{\Omega_{shear}}{c/r_j}\right)^{-2}\left(\frac{\lambda_f(p)}{\rm kpc}\right)^{-1}$$

Webb et al 2018, Reiger 2019

nonGradual Shear Acc

$$t_{\rm nGSA} \sim \zeta\frac{\lambda_f}{c\Gamma_z^2\,\beta_z^2}$$

Kimura et al 2018, Caprioli 2015

Turbulent Shear Acc

$$t_{\rm TSA} = 2.88\times10^4{\rm yr}\left(\frac{L_0/\gamma}{1{\rm kpc}}\right)^{\frac{2}{3}}\left(\frac{|v_{tur}|}{c}\right)^{-2}\left(\frac{\lambda_f(p)}{\rm kpc}\right)^{1/3}$$

Ohira 2013

diffusive escape time

$$t_D \sim \frac{(\frac{W}{2})^2}{c\,\lambda_f}$$

diffusion time across the cocoon with a width W

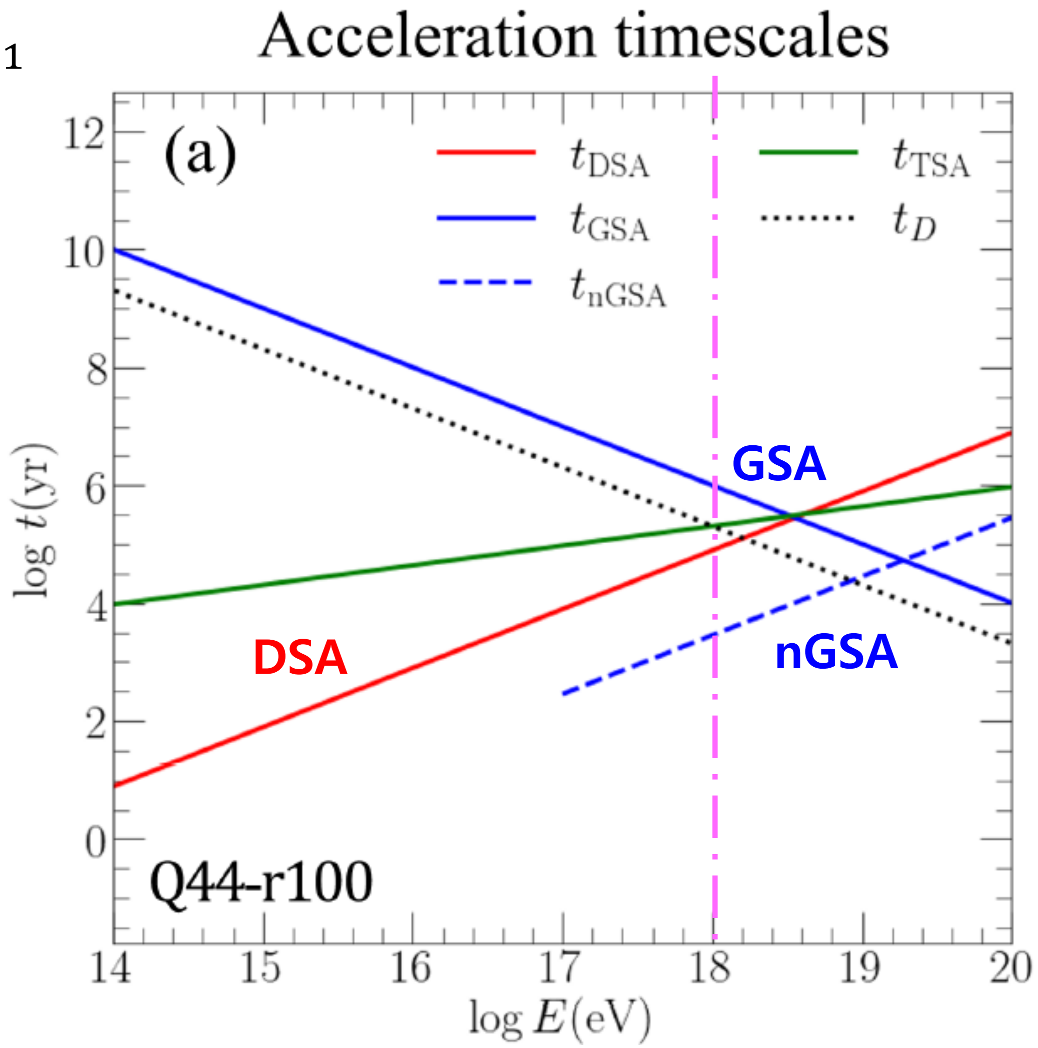

different APs in typical jet flows

Seo et al. 2023a

Relative importance of acceleration processes: approximate estimation

At each scattering event, relative contribution of acceleration processes (APs) in the bin of $[\log E\,, \log E + d\log E]$

$$\xi_{\rm AP} = t_{\rm AP}^{-1} / \sum_{\rm AP} t_{\rm AP}^{-1}$$

$$\mathcal{E}_{\rm AP}(E) = \frac{\sum_{\log E}^{\log E + d\log E} \xi_{\rm AP} \Delta E}{\sum_{\log E}^{\log E + d\log E} \Delta E}$$

$\Delta E = E_{\rm after} - E_{\rm before}$

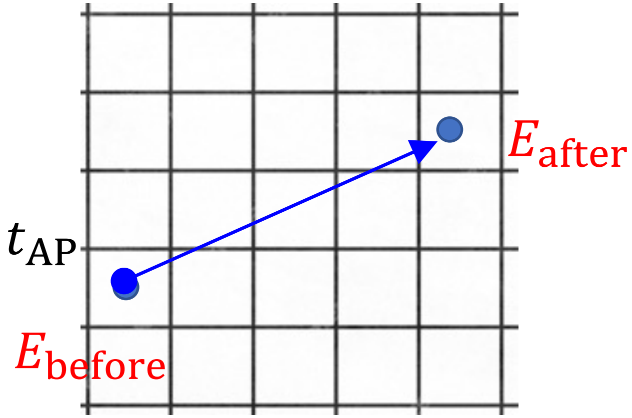

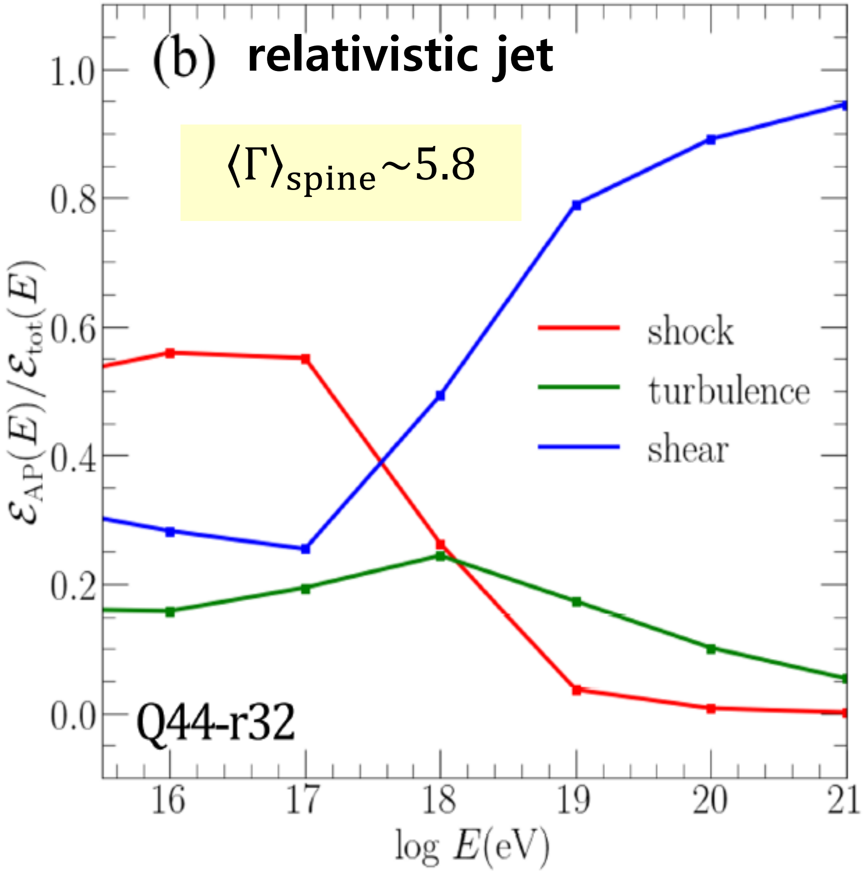

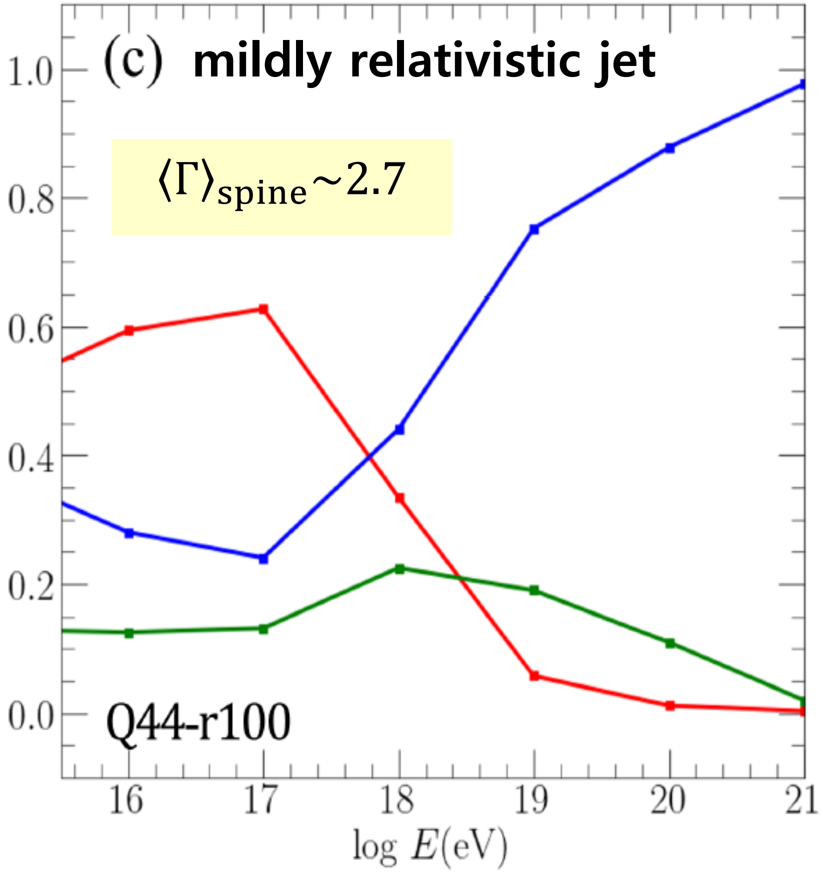

- **Shock acceleration is the main acceleration for *E* < ~EeV.**
- **Shear acceleration is the primary mechanism for *E* > ~EeV.**
- **Turbulence acceleration plays a secondary role.**

Evolution toward time-asymptotic energy spectrum of escaping CRs

Transition from ``age-limited" to ``size-limited" spectrum: $r_j = 1\text{kpc}$ $t_{cross} \sim 10^4 - 10^5\ yr$

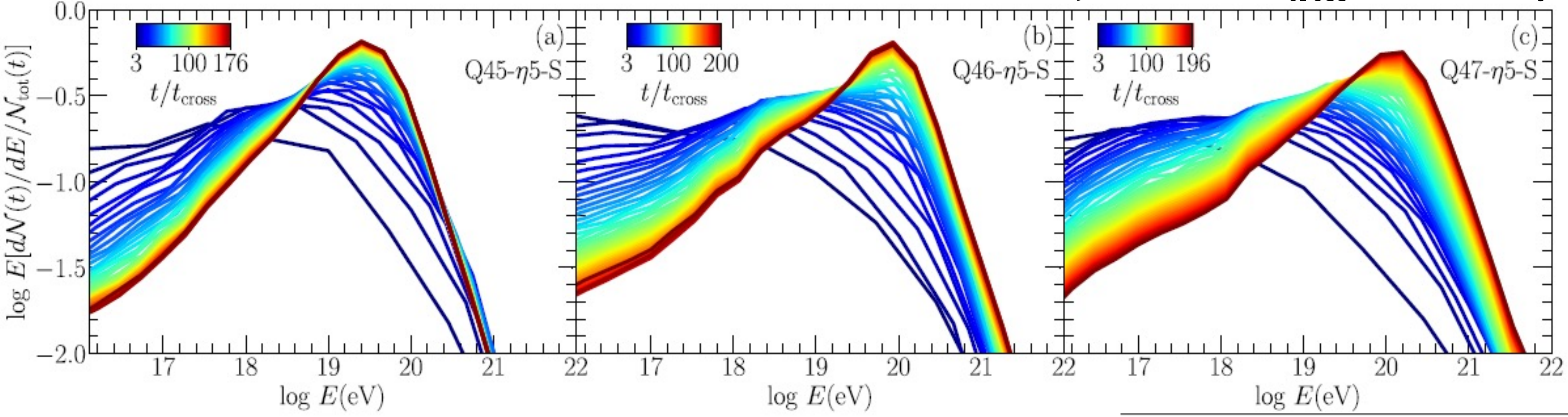

$r_j = 1\text{kpc}$

Model Name[a]	Q_j(erg s^{-1})	Γ_j	t_{cross}(yr)
Q45-η5-S	3.34E+45	7.2644	7.97E+4
Q46-η5-H	3.34E+46	22.5645	2.77E+4
Q46-η5-S	3.34E+46	22.5645	2.77E+4
Q46-η5-L	3.34E+46	22.5645	2.77E+4
Q47-η5-S	3.34E+47	71.0149	1.10E+4

$r_j = 10\text{pc}$, $r_j = 100\text{pc}$

Model name[c]	Q_j (erg s^{-1})	r_j (pc)	Γ_j	t_{cross} (yrs)
Q42-r10	3.5E42	10	3.9	2.5E3
Q43-r10	3.5E43	10	11.2	8.6E2
Q44-r10	3.5E44	10	34.5	3.0E2
Q43-r32	3.5E43	31.6	3.9	7.9E3
Q44-r32	3.5E44	31.6	11.2	2.7E3
Q45-r32	3.5E45	31.6	34.5	9.5E2
Q44-r100	3.5E44	100	3.9	2.5E4
Q45-r100	3.5E45	100	11.2	8.6E3

Energy spectrum of escaping particles

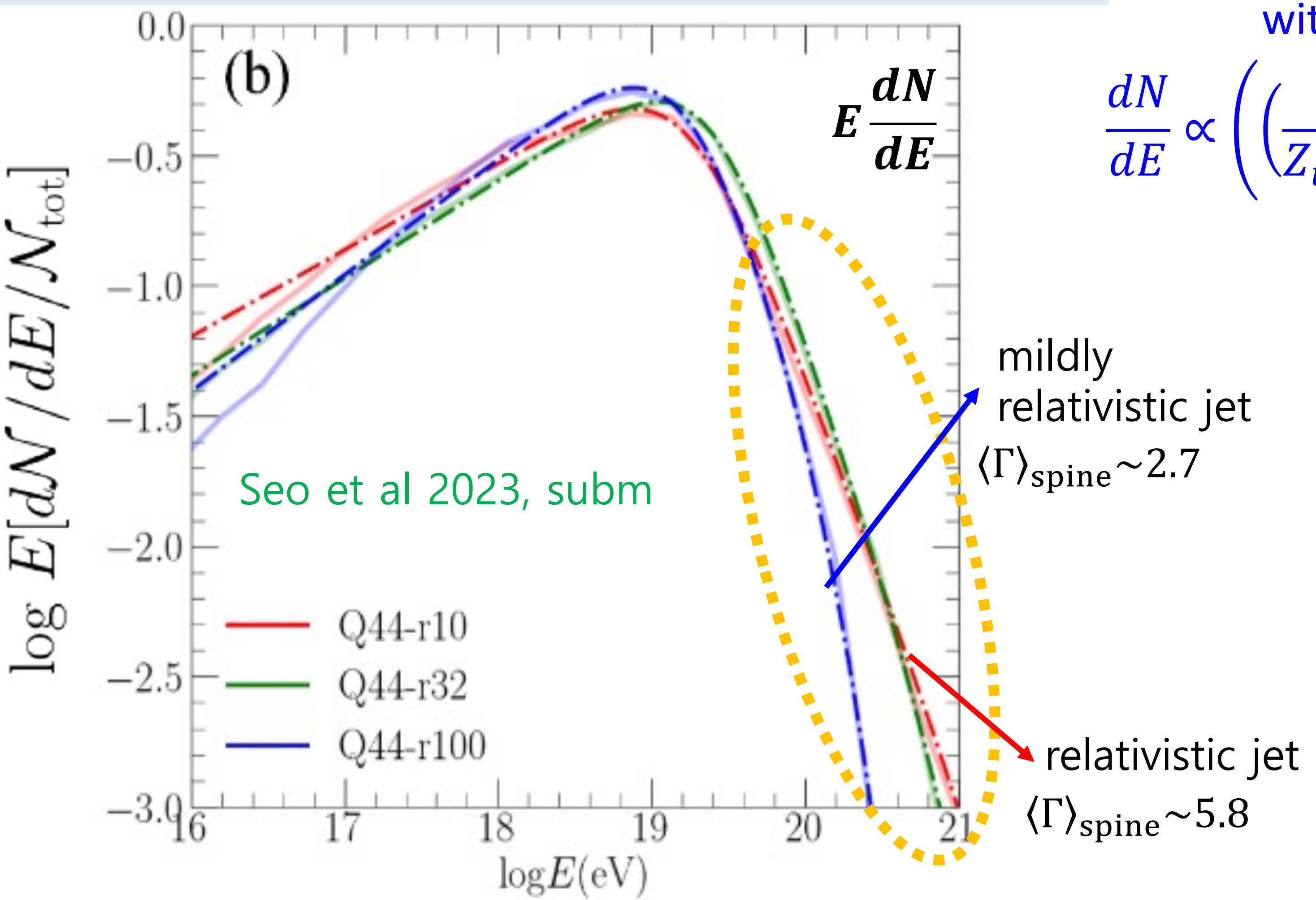

double power law
with an extended exponential cutoff

$$\frac{dN}{dE} \propto \left(\left(\frac{E}{Z_i E_{break}}\right)^{-s_1} + \left(\frac{E}{Z_i E_{break}}\right)^{-s_2}\right)^{-1}$$

$$\times \exp\left(-\frac{E}{Z_i E_{break} \langle\Gamma\rangle^2_{spine}}\right)$$

- $E < Z_i E_{break}$: $dN/dE \propto E^{-0.6}$

due to **shear acceleration**
cf. Ostrowski 1998
Kimura et al 2018

- $E > Z_i E_{break}$: $dN/dE \propto E^{-2.6}$

controlled by the confinement within an elongated cocoon

- $Z_i E_{break}$: **depends mainly on the jet power Q_j**
- Exponential cutoff at $Z_i E_{break} \langle\Gamma\rangle^2_{spine}$
- $\langle\Gamma\rangle_{spine}$ is the mean Lorentz factor of the jet-spine flow

Why double power law ? How to model Break Energy ?

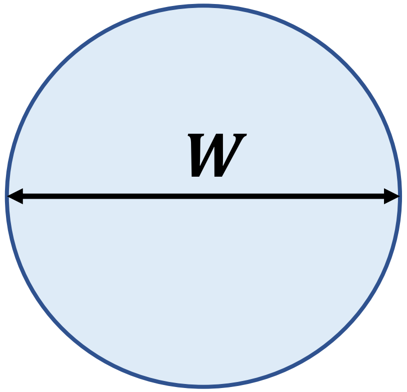

Sphere → single power-law with a cutoff

Hillas Energy: $E_H \approx 0.9\ EeV \left(\frac{\langle B \rangle}{1\mu G}\right)\left(\frac{0.5W}{1kpc}\right)$

$E_{\rm break} \sim E_H$ by confinement condition

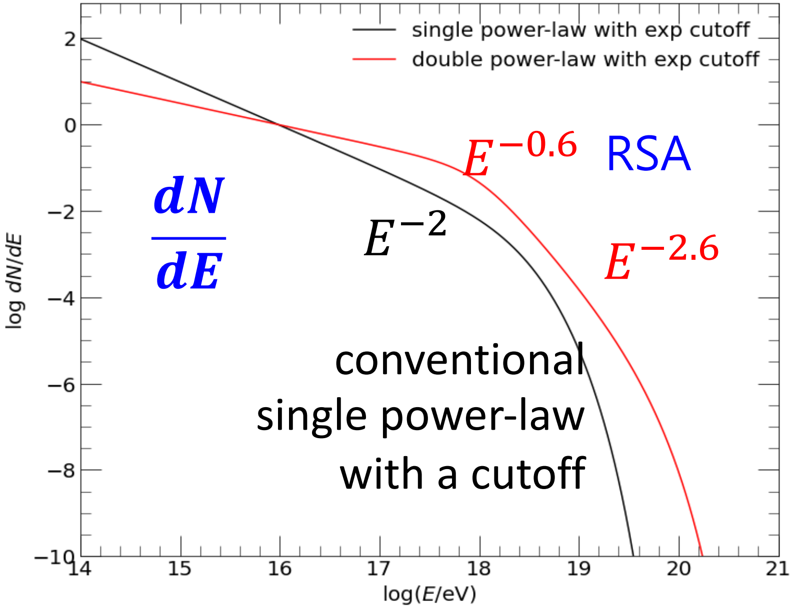

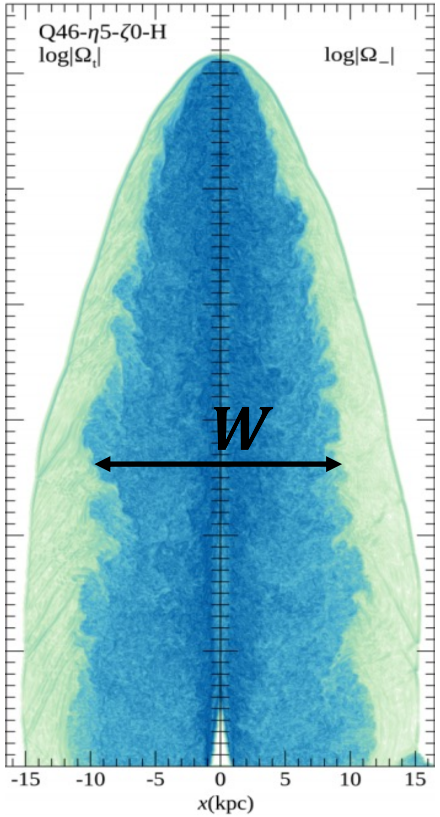

Elongated cylinder (cocoon)→ double power-law with a cutoff

If $t_{\rm nGSA} < t_D$, $E_{\rm break} \sim E_H$ Jets with larger $\langle \Gamma_j \rangle$

E_{max} is limited by the **confinement** condition.

If $t_{\rm nGSA} > t_D$, $E_{\rm break} \sim E_D$ Jets with smaller $\langle \Gamma_j \rangle$

E_{max} is limited by the **diffusive escape**.

$t_{\rm nGSA} = t_D$ $\zeta \frac{\lambda_f}{c\Gamma_z^2\,\beta_z^2} \sim \frac{(W/2)^2}{c\,\lambda_f}$

$E_D \approx E_H \langle \Gamma_z \beta_z \rangle_{\rm acc} \sim \varphi E_H$

$\varphi \sim 0.3 - 1.0$

Application of our model spectrum to reproduce observations of UHECRs

Seo et al. in prep

- **Model Source Spectrum at RGs**

$$\frac{dN}{dE_0 dt} = S_0 \left(\left(\frac{E_0}{Z_0 E_b(Q_j)} \right)^{-s_1} + \left(\frac{E_0}{Z_0 E_b(Q_j)} \right)^{-s_2} \right)^{-1} \exp\left(-\frac{E_0}{Z_0 \langle \Gamma_j \rangle^2 E_b(Q_j)} \right)$$

where Q_j, Γ_j, E_0, Z_0, and S_0 represent the jet power, the Lorentz factor of the jet, the energy of the particle, the charge of the particle, and the normalization factor of the source function

- **Model for Break energy:** $E_b(Q_j) = \xi \cdot \varphi \cdot E_H \cdot (Q_j/Q_n)^{\alpha}$

Our RHD & MC simulation results suggest

$Q_n \approx 3.5 \times 10^{44}$ erg/s, $E_H \approx 1.5 \times 10^{19}$ eV, $\xi \sim 1$

$\langle \Gamma_j \rangle \approx 2$ for FR-I & $\langle \Gamma_j \rangle \approx 10$ for FR-II,

$\alpha \approx 1/4$ for FR-I & $\alpha \approx 1/3$ for FR-II,

$\varphi \sim 0.3 - 1$ (depending on $\langle \Gamma_j \rangle$)

- **Chemical abundance**: 3 x Galactic values (elliptical galaxies) e.g. Kimura et al. 2018

Propagation of UHECRs from RGs to Earth

R. Alves Batista, et al. JCAP (2022) no. 09, 035

https://crpropa.desy.de/

In **CRPropa3** simulations, we include the following modules:

- photo-pion Production
- photodisintegration
- electron pair production
  by CMB and extragalactic background light (Gilmore et al. 2012)
- redshift evolution (adiabatic energy loss)

Modeling the contribution from radio galaxies (RGs)

- The total energy of escaped CR particles is proportional to the radio luminosity of RGs. (Godfrey & Shabala, 2013)

$$Q_{\mathrm{FR-I}} = 5\times10^{44}\left(\frac{L_{151}}{10^{25}\mathrm{W\,Hz}^{-1}\,\mathrm{sr}^{-1}}\right)^{0.64} \qquad Q_{\mathrm{FR-II}} = 1.5\times10^{44}\left(\frac{L_{151}}{10^{25}\mathrm{W\,Hz}^{-1}\,\mathrm{sr}^{-1}}\right)^{0.67}$$

- **Modeling for the Lorentz factor** for cosmological RG sources ($0.1 \lesssim z \lesssim 1$)

$$\Gamma_c(Q_j, q) = \Gamma_{\min}(Q_j/Q_{\min})^q \qquad Q_{\min} = 10^{42}\ \mathrm{erg/s} \qquad q_1 = 1/5 \text{ for FR-I};\ q_2 = 1/3 \text{ for FR-II}$$

UHECRs from nearby RG jets

e.g. Virgo A, Cen A

abundance: 3 x Galactic values (elliptical galaxies) e.g. Kimura + 2018

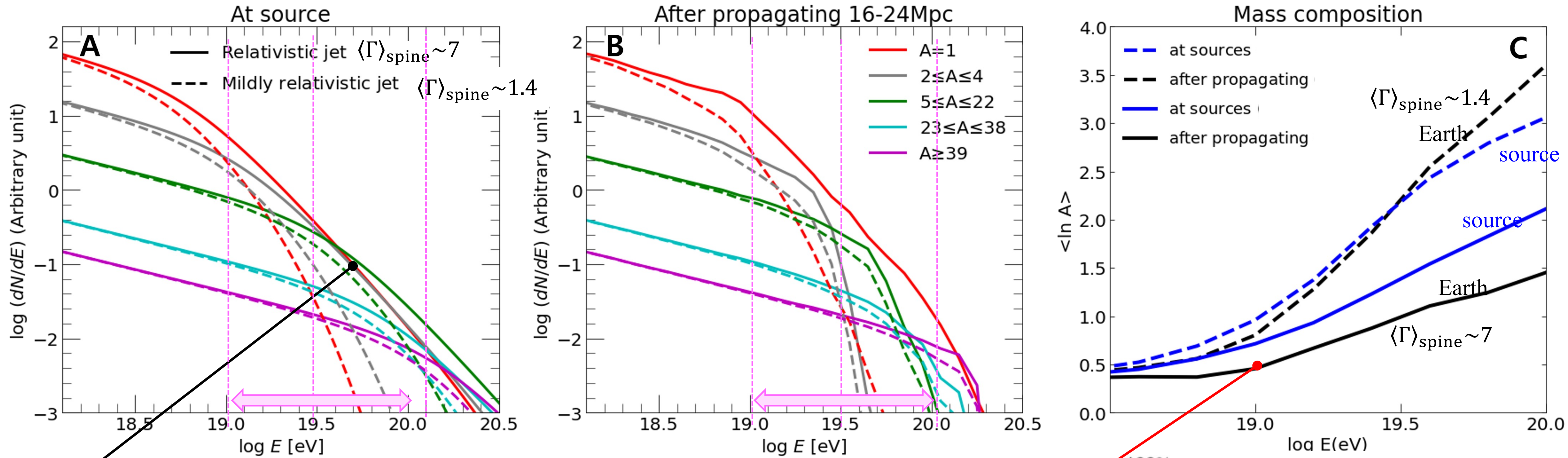

- **Jets with higher Γ (solid lines) generate more UHECRs flux for E>10EeV**
- **UHECRs from jets with higher Γ (solid lines) have a smaller <ln A>, i.e., lighter composition for E=10-100EeV.**
- **The mass composition of arrived UHECRs could become heavier or lighter, depending on Γ, chemical composition, propagation distance, etc.**

Seo et al. in prep

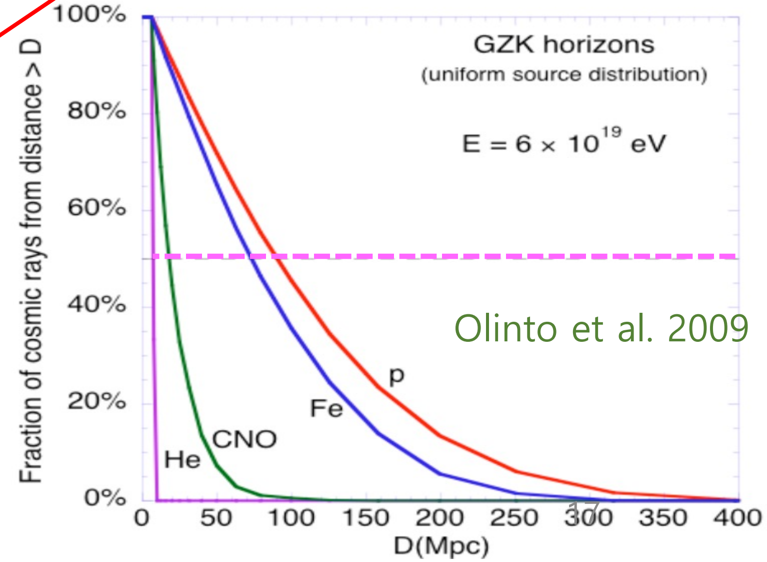

Olinto et al. 2009

Energy spectrum & mass composition of UHECRs from radio galaxy jets

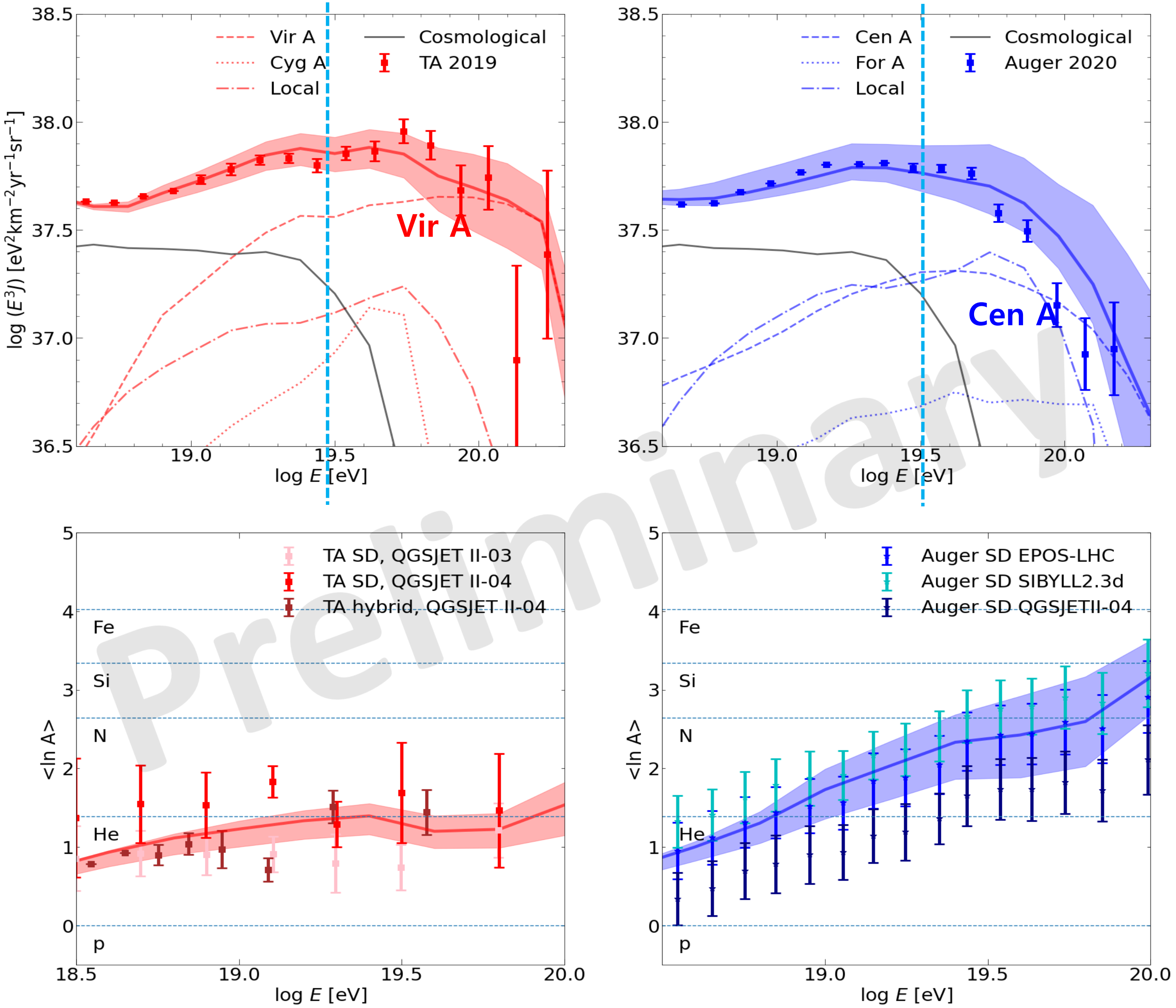

Shading represents ± 20 % variations of model parameters.

Seo et al. in prep

- **Virgo A** with $<\Gamma>\sim 7$, may account for a substantial fraction of the observed at **TA**.
- **Cen A** with $<\Gamma>\sim 1.2$ along with local RGs may account for a substantial fraction of the UHECRs observed at **Auger.**
- The Lorentz factor of RG jets affects the mass composition, $\langle \ln A \rangle$, of UHECRs observed at Earth as well as at sources.

Source Modeling: 3 components

1. major RGs:
   Centaurus A, Fornax A for TA
   Virgo A, Cygnus A for Auger
2. Local RGs (d<300 Mpc):
   Rachen & Eichmann 2019
3. Cosmological Sources: $0.1 \lesssim z \lesssim 1$
   Mingo et al. 2018

Summary

- The energy spectrum of the UHECRs produced at radio galaxies (RGs) could be modeled as a double power law with an extended exponential cutoff, thanks to RHD & MC simulations. However, a better understanding of the detailed physical processes is crucial.
- Compared to a single power-law with an exponential cutoff at Hillas energy, our source spectrum model results in an observed UHECR spectrum that may extend to higher E and has a lighter $\langle \ln A \rangle$ at the highest E.
- Understanding the proprieties of local RGs, such as the Lorentz factor Γ_j, jet power Q_j, radius r_j, magnetic field B, & age of the jet, would be important in modeling the observations of UHECRs.

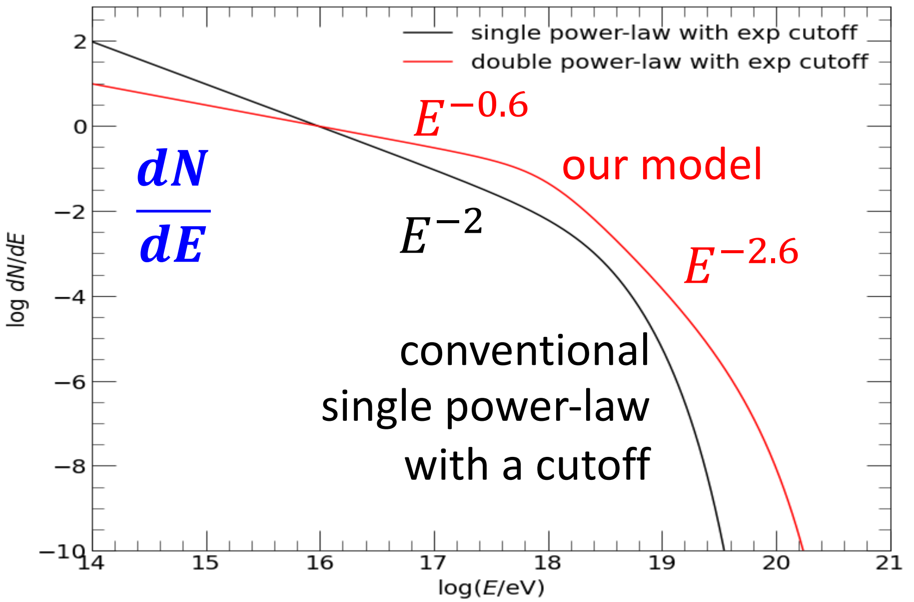

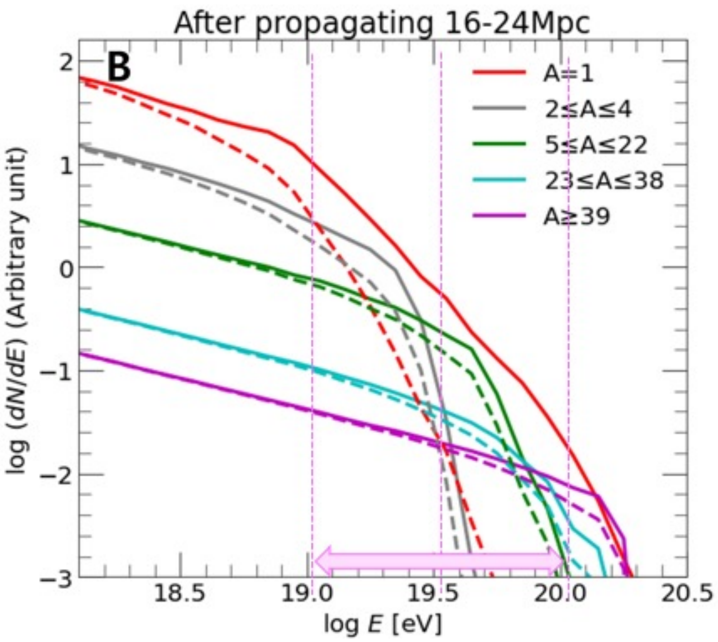

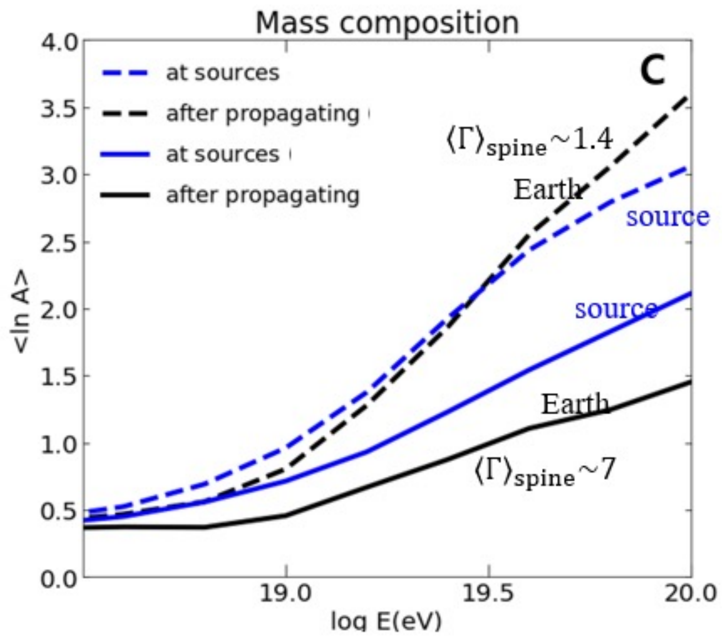

Supplementary Materials

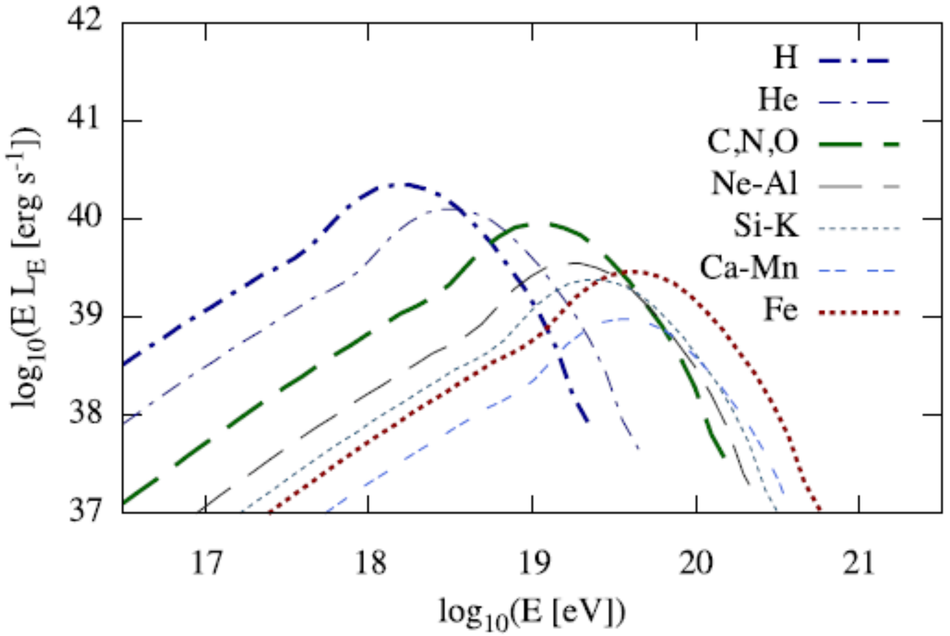

Kimura et al. 2018

“the shear reacceleration mechanism leads to a hard spectrum of escaping cosmic rays, dLE/dE ∝ $E^{-1} - E^{0}$, distinct from a conventional E^{-2} spectrum.”

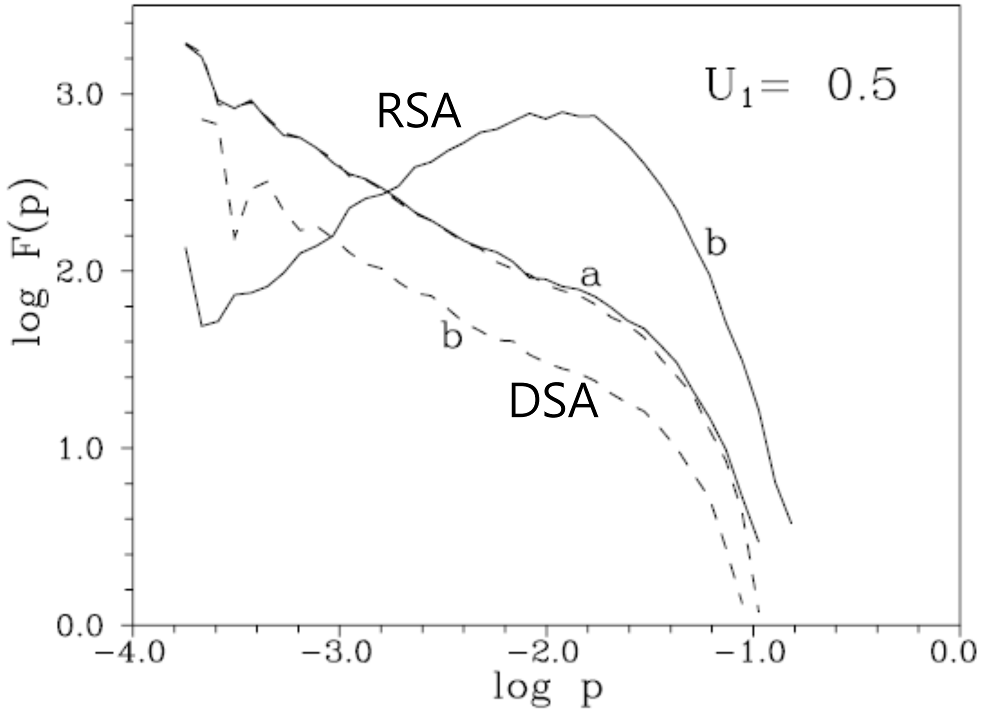

Ostrowski 19998

“the spectrum of particles accelerated at the jet side boundary is expected to be much flatter than the one formed at the shock.”

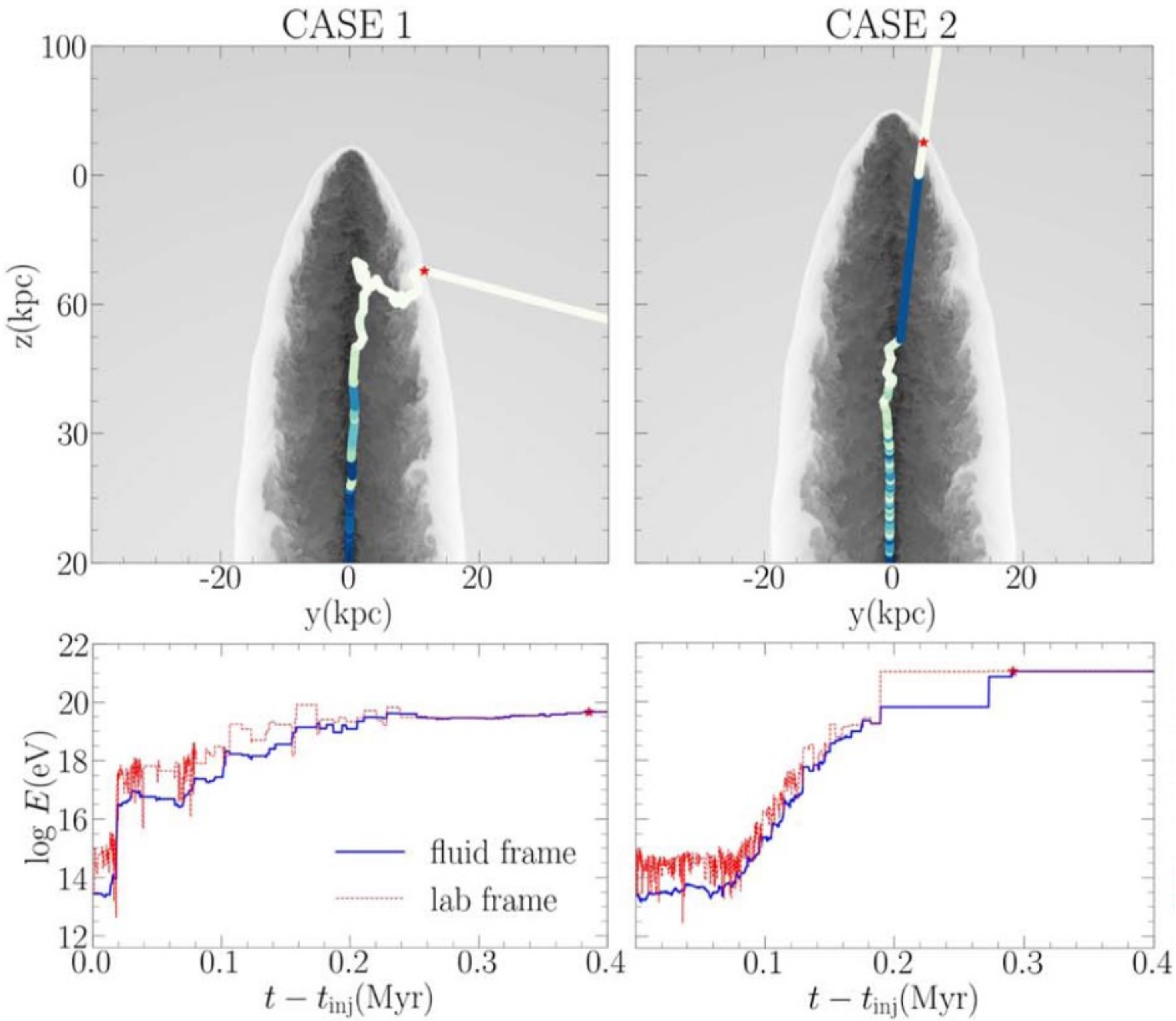
CASE 1
CASE 2
z(kpc)
y(kpc)
log E(eV)
$t - t_{\rm inj}$(Myr)
fluid frame
lab frame

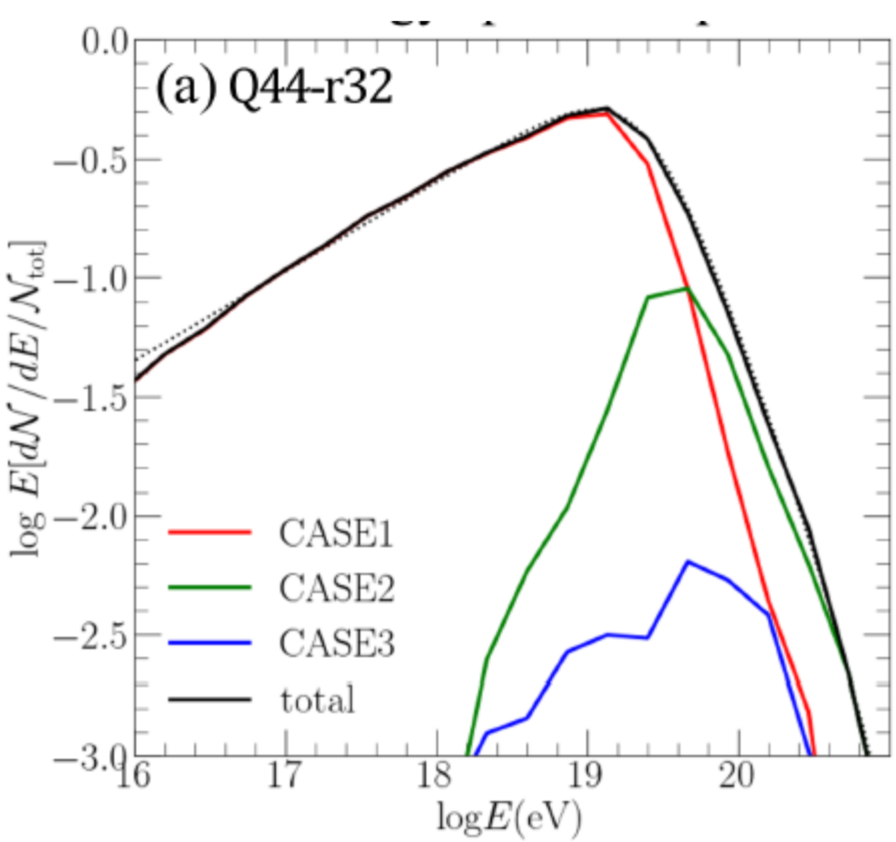
(a) Q44-r32
$\log E[dN/dE/N_{\rm tot}]$
CASE1
CASE2
CASE3
total
log E(eV)

Table 1
Simulation Models for FR-II Jets

Model Name[a]	Q_j(erg s^{-1})	$\eta \equiv \frac{\rho_j}{\rho_b}$	$\dot{M}_j$(dyne)	u_j/c	Γ_j	$u^*_{\rm head}/c$	$t_{\rm cross}$(yr)	Grid Zones	$N_j \equiv \frac{r_j}{\Delta x}$ [b]	$\frac{t_{\rm end}}{t_{\rm cross}}$
Q45-η5-S	3.34E+45	1.E-05	1.15E+35	0.9905	7.2644	0.0409	7.97E+4	$(400)^2 \times 600$	5	176
Q46-η5-H	3.34E+46	1.E-05	1.13E+36	0.9990	22.5645	0.1180	2.77E+4	$(800)^2 \times 1200$	10	111
Q46-η5-S	3.34E+46	1.E-05	1.13E+36	0.9990	22.5645	0.1180	2.77E+4	$(400)^2 \times 800$	5	200
Q46-η5-L	3.34E+46	1.E-05	1.13E+36	0.9990	22.5645	0.1180	2.77E+4	$(240)^2 \times 360$	3	150
Q47-η5-S	3.34E+47	1.E-05	1.12E+37	0.9999	71.0149	0.2965	1.10E+4	$(400)^2 \times 1000$	5	196

Table 1. Model Parameters of Simulated Jets[a] and Fitting Parameters for UHECR Energy Spectrum[b]

Model name[c]	Q_j (erg s^{-1})	r_j (pc)	Γ_j	r_c (pc)	$t_{\rm cross}$ (yrs)	$t_{\rm end}$ ($t_{\rm cross}$)	s_1	s_2	$E_{\rm break}$ (eV)	$\Gamma_{\rm fit}$	E_H[d] (eV)	E_D[d] (eV)	$\langle\Gamma\rangle_{\rm spine}$[d]
Q42-r10	3.5E42	10	3.9	uniform	2.5E3	50	-0.60	-2.50	2.6E18	2.8	4.6E18	2.3E18	2.8
Q43-r10	3.5E43	10	11.2	uniform	8.6E2	50	-0.61	-2.65	7.5E18	7.1	8.2E18	7.4E18	6.0
Q44-r10	3.5E44	10	34.5	uniform	3.0E2	75	-0.64	-2.57	1.7E19	15.5	1.5E19	2.3E19	13.4
Q43-r32	3.5E43	31.6	3.9	400	7.9E3	50	-0.56	-2.51	5.7E18	2.5	1.5E19	6.0E18	2.7
Q44-r32	3.5E44	31.6	11.2	400	2.7E3	50	-0.62	-2.70	2.3E19	6.4	2.6E19	2.2E19	5.8
Q45-r32	3.5E45	31.6	34.5	400	9.5E2	65	-0.60	-2.35	4.3E19	15.2	4.6E19	6.4E20	12.9
Q44-r100	3.5E44	100	3.9	1200	2.5E4	50	-0.56	-2.51	1.7E19	2.5	4.6E19	1.8E19	2.7
Q45-r100	3.5E45	100	11.2	1200	8.6E3	50	-0.62	-2.70	7.0E19	6.4	8.2E19	7.0E19	5.8

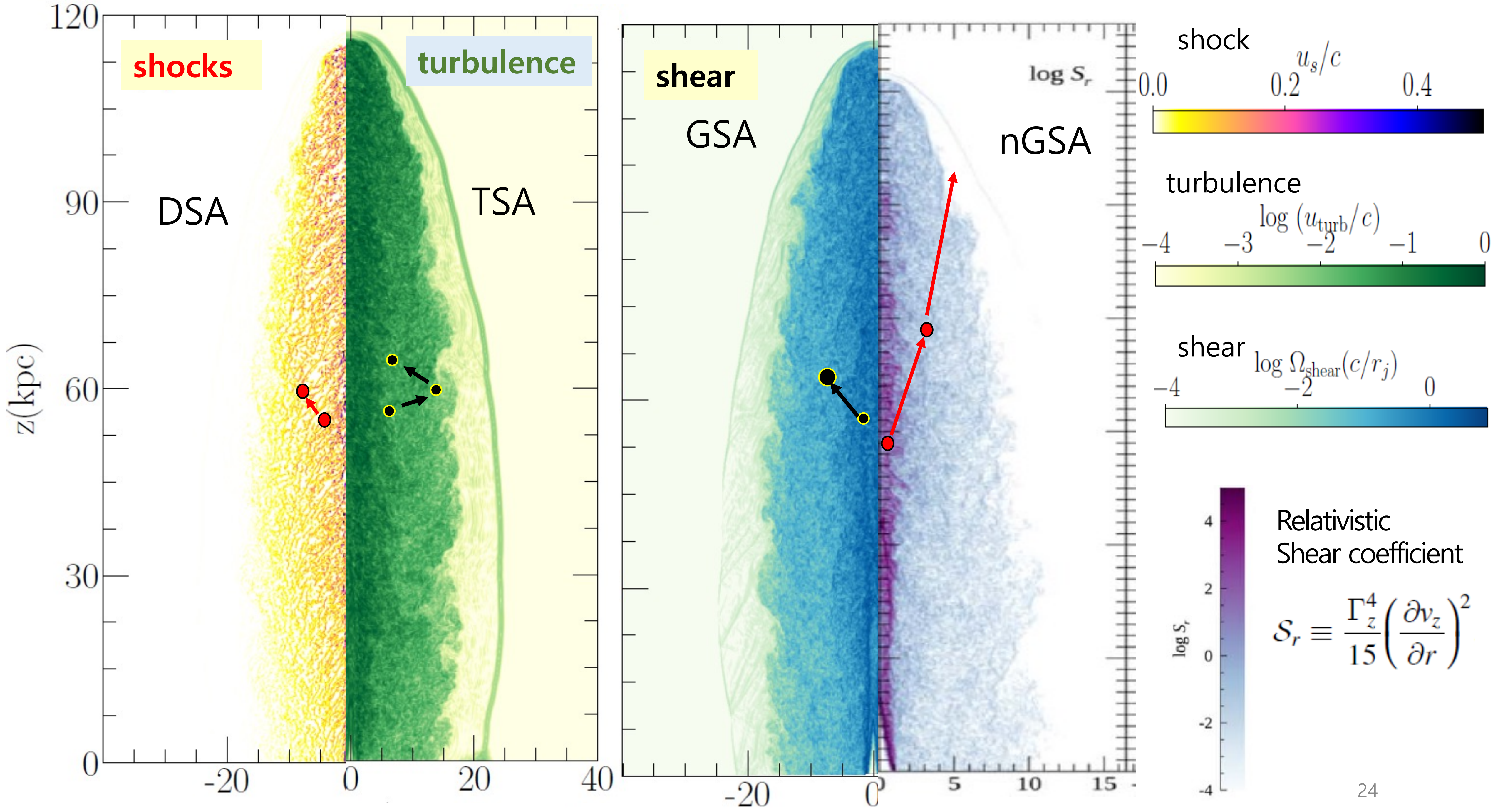
shocks
turbulence
DSA
TSA
shear
GSA
nGSA
log S_r
z(kpc)
shock
u_s/c
turbulence
log (u_{turb}/c)
shear
log $\Omega_{shear}(c/r_j)$
log S_r
Relativistic
Shear coefficient
$$S_r \equiv \frac{\Gamma_z^4}{15}\left(\frac{\partial v_z}{\partial r}\right)^2$$